Adhesion-induced lateral phase separation of multicomponent membranes: The effect of repellers and confinement

Mesfin Asfaw* and Hsuan-Yi Chen
Department of Physics and Institute of Biophysics, National Central University, Jhongli 32001, Taiwan
(Received 19 November 2008; revised manuscript received 25 February 2009; published 20 April 2009)

We present a theoretical study of adhesion-induced lateral phase separation for a membrane with short stickers, long stickers, and repellers confined between two hard walls. The effects of confinement and repellers on lateral phase separation are investigated. We find that the critical potential depth of the stickers for lateral phase separation increases as the distance between the hard walls decreases. This suggests confinement-induced or force-induced mixing of stickers. We also find that repellers with stronger repulsive potential tend to enhance, while repellers with weaker repulsive potential tend to suppress adhesion-induced lateral phase separation.

DOI: 10.1103/PhysRevE.79.041917 PACS number(s): 87.16.D−, 82.40.Np, 68.35.Np, 05.40.−a

I. INTRODUCTION

Biological membranes are lipid bilayers with different types of embedded or absorbed macromolecules. They serve a number of general functions in our cells and tissues [1,2]. Because of its biological importance, the physics of membrane adhesion has received considerable attention both theoretically and experimentally [3–10]. For instance, helper T cells mediate immune responses by adhering to antigen-presenting cells (APCs) which exhibit foreign peptide fragments on their surface [11]. The APC membranes contain the ligands MHCp and ICAM-1, while the T cells contain the receptors TCR and LFA-1. The experiments [11] show the formation of domains into shorter TCR/MHCp receptor-ligand complexes and the longer LFA-1/ICAM-1 receptor-ligand complexes. The dynamics of adhesion-induced phase separation has been studied theoretically [12–14]. For example, the Monte Carlo study by Weikl and Lipowsky [14] showed that the height difference between different junctions causes a lateral phase separation, and the formation of targetlike immunological synapse is assisted by the motion of cytoskeleton.

The equilibrium studies of adhesion-induced phase separation of multicomponent membranes are also important for a complete understanding of the physics of membrane adhesion. For instance, in recent papers [15,16], the general case of two membranes binding to each other with two types of stickers is considered and the equilibrium phase behavior of such a system is studied at the mean-field and Gaussian level by including the effects of sticker flexibility difference, sticker height difference, and thermally activated membrane height fluctuations. More recently, Asfaw *et al.* [17] presented a theoretical study that characterized the phase diagram and the scaling laws for the critical potential depth of unbinding and lateral phase separation. These studies show that membranes are unbound for small potential depths and bound for large potential depths. In the bound state, the length mismatch leads to a membrane-mediated repulsion between stickers of different lengths and this leads to lateral phase separation depending on the concentrations and strengths of the receptor-ligand bonds. Furthermore, the flexibilities of the stickers play nontrivial roles in the location of phase boundaries.

Most of these recent works deal with membranes with one or two types of stickers. However, biological membranes usually contain glycoproteins which are repulsive to another membrane or tissue; i.e., they act as repellers. This important fact motivates us to study adhesion-induced lateral phase separation of membranes with short stickers, long stickers, and repellers. Another important but unexplored issue on adhesion-induced lateral phase separation in biomembranes is the effect of external pressure or confinement on the phase diagram. For example, cell adhesions often occur in the presence of external force field due to external flow, or the external force may be a result of the occurrence of cell adhesions in highly confined geometry during the development of multicellular organisms. To study the effect of repellers and confinement on adhesion-induced lateral phase separation, in this paper we first consider a membrane with short stickers and long stickers which are in contact with another planer surface (substrate) in the absence of repellers. The membrane and the substrate are confined between two hard walls. We find that the critical binding energies of the stickers for lateral phase separation increase as the distance between the hard walls decreases due to the steric repulsion of the membrane with the hard walls. Then the effects of repellers are considered and we find that repellers with strong repulsive potential tend to enhance phase separation, while repellers with weak repulsive potential tend to suppress phase separation. Our study has revealed the possibility of manipulating the lateral distribution of stickers in future experiments.

This paper is organized as follows. In Sec. II we present the model of membranes with short stickers, long stickers, and repellers. By tracing out sticker and repeller degrees of freedom, we get membranes that interact with an effective double-well potential. The adhesion-induced lateral phase separation in the presence of stickers and repellers is studied by mean-field theory and Monte Carlo simulations in Sec. III. First we consider membranes without repellers to study the effect of confinement on the phase behavior of the system. After that we study how repellers affect the state of the

*Present address: APCTP, Pohang 790-784, Korea.

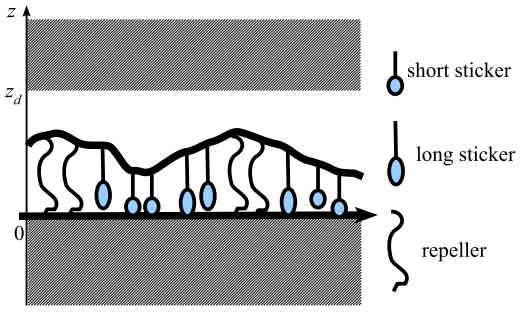

FIG. 1. (Color online) Schematic figure of a membrane with short stickers, long stickers, and repellers confined vertically between a substrate and an upper surface. The upper surface is located at a distance z_d above the substrate.

system. Section IV is the summary and conclusion.

II. MODEL

We consider a tensionless multicomponent membrane with short and long receptor-ligand bonds that interacts with a substrate as shown in Fig. 1. Let us denote the short and long receptor-ligand bonds as short and long stickers, respectively. To study the effect of confinement on the system, we include a fixed upper surface at a distance z_d from the substrate. In our model, the membrane is discretized into a two-dimensional square lattice with lattice constant a [8,17]. We choose $a=6$ nm, the smallest length scale for membrane continuum elasticity theory to be valid. The separation field $l \geq 0$ describes the vertical distance between the membrane and the substrate. An additional field $n_i=0$, 1, 2, or 3 denotes the occupation state of the ith site. $n_i=0$ indicates the absence of stickers and repellers at lattice site i, while $n_i=1$ (2) denotes the presence of a type-1 (2) sticker at lattice site i. $n_i=3$ denotes the presence of a repeller at a site i.

The grand canonical Hamiltonian of the system under consideration is given by

$$H[l,n] = H_{el}[l] + \sum_i \delta_{1,n_i}[V_1(l_i) - \mu_1] + \sum_i \delta_{2,n_i}[V_2(l_i) - \mu_2] + \sum_i \delta_{3,n_i}[V_3(l_i) - \mu_3]. \tag{1}$$

here $H_{el}[l]=\Sigma_i \frac{\kappa}{2a^2}(\Delta_d l_i)^2$ denotes the discretized bending energy of the membrane with bending rigidity κ. The typical magnitude of κ is $(10-20)k_BT$. The discretized Laplacian Δ_d is given by $\Delta_d l_i = l_{i1}+l_{i2}+l_{i3}+l_{i4}-4l_i$, where l_{i1} to l_{i4} are the four nearest-neighbor membrane separation fields of the membrane patch i. The second and third terms on the right-hand side of Eq. (1) are interaction potentials between the stickers and the substrate. μ_1 and μ_2 denote the chemical potentials of stickers 1 and 2, respectively. The parameters $V_3(l_i)$ and μ_3 represent potentials and the chemical potentials of the repellers, respectively. We consider the following sticker potentials: for $\alpha=1,2$,

$$V_\alpha = \begin{cases} U_\alpha & \text{if } l_\alpha < l < l_\alpha + l_{we\alpha} \\ 0 & \text{otherwise,} \end{cases} \tag{2}$$

where U_1 and U_2 are both negative and $l_1 < l_2$. That is, type-1 stickers are shorter than type-2 stickers. The repulsive potential of the repellers is $V_3=U_3>0$ for $0<l<l_3$.

The equilibrium properties of the system can be obtained from the grand partition function Z,

$$Z = \prod_i \int_0^{z_d} dl_i \sum_{n_i=0}^{3} \exp\left[\frac{-H[l,n]}{k_BT}\right]. \tag{3}$$

Absorbing the Boltzmann constant k_B into the temperature T and tracing out the sticker degrees of freedom, one gets

$$\begin{aligned} Z &= \int_0^{z_d} \prod_i dl_i \exp[-H_{el}(l)] \left\{ 1 + \exp\left[\frac{-V_1(l_i)+\mu_1}{T}\right] + \exp\left[\frac{-V_2(l_i)+\mu_2}{T}\right] + \exp\left[\frac{-V_3(l_i)+\mu_3}{T}\right] \right\} \\ &= \int_0^{z_d} dl_i \prod_i \exp\left[\frac{-H_{el}(l) + \sum_i V^{\text{eff}}(l_i)}{T}\right], \end{aligned} \tag{4}$$

where the effective potential $V^{\text{eff}}(l)$ is given by

$$V^{\text{eff}} = \begin{cases} U_{ba} & \text{for } 0 < l < l_1 \\ U_1^{\text{eff}} & \text{for } l_1 < l < l_1 + l_{we1} \\ U_{ba} & \text{for } l_1 + l_{we1} < l < l_2 \\ U_2^{\text{eff}} & \text{for } l_2 < l < l_2 + l_{we2} \\ U_{ba} & \text{for } l_{we2} < l < l_3 \\ 0 & \text{otherwise,} \end{cases} \tag{5}$$

where

$$U_1^{\text{eff}} = -T \ln\left[\frac{1 + \exp\left[\frac{-U_1+\mu_1}{T}\right] + \exp\left[\frac{\mu_2}{T}\right] + \exp\left[\frac{\mu_3}{T}\right]}{1 + \exp\left[\frac{\mu_1}{T}\right] + \exp\left[\frac{\mu_2}{T}\right] + \exp\left[\frac{\mu_3}{T}\right]}\right], \tag{6}$$

$$U_2^{\text{eff}} = -T \ln\left[\frac{1 + \exp\left[\frac{\mu_1}{T}\right] + \exp\left[\frac{-U_2+\mu_2}{T}\right] + \exp\left[\frac{\mu_3}{T}\right]}{1 + \exp\left[\frac{\mu_1}{T}\right] + \exp\left[\frac{\mu_2}{T}\right] + \exp\left[\frac{\mu_3}{T}\right]}\right], \tag{7}$$

and

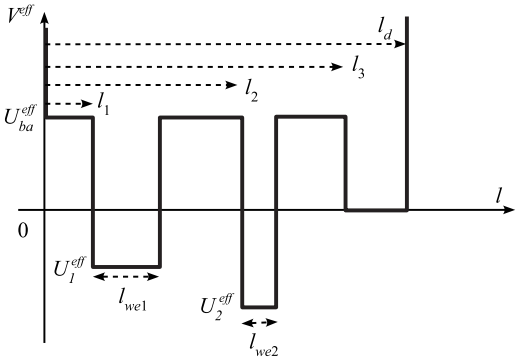

FIG. 2. Schematic effective potential V^{eff} versus l. The potential has two square wells of depths $|\bar{U}_1^{\text{eff}}|$ and $|\bar{U}_2^{\text{eff}}|$ and widths l_{we1} and l_{we2}, respectively. There is a barrier U_{ba}^{eff} due to the repellers and a hard wall located at l_d which represents the upper surface.

$$U_{ba}^{\text{eff}} = -T\ln\left[\frac{1+\exp\left[\frac{\mu_1}{T}\right]+\exp\left[\frac{\mu_2}{T}\right]+\exp\left[\frac{-U_3+\mu_3}{T}\right]}{1+\exp\left[\frac{\mu_1}{T}\right]+\exp\left[\frac{\mu_2}{T}\right]+\exp\left[\frac{\mu_3}{T}\right]}\right], \tag{8}$$

as shown in Fig. 2.

In Sec. III, the phase behavior of membranes under the effective potential given by Eq. (5) will be studied by mean-field approximation and Monte Carlo simulations.

III. MEAN-FIELD THEORY AND MONTE CARLO SIMULATION

It is convenient to introduce the rescaled separation field $z=(l/a)\sqrt{\kappa/T}$ and the rescaled effective potential $\bar{V}^{\text{eff}}=V^{\text{eff}}/T$. In equilibrium state the rescaled separation field z fluctuates around its average value $z_{\min}$. When the fluctuation is not very strong, mean-field approximation can be applied to the discretized Laplacian such that $H_l[z]=\Sigma_i(4[z_{\min}-z_i])^2$. In this approximation z_i at different sites are decoupled. Hence Eq. (4) becomes

$$Z=\left\{\int_0^{z_d} dz\,\exp[-8(z_{\min}-z)^2-\bar{V}^{\text{eff}}(z)]\right\}^N, \tag{9}$$

and the mean-field free energy of the membrane is given by

$$G=-NT\ln\left(\int_0^{z_d} dz\{\exp[-8(z_{\min}-z)^2-\bar{V}^{\text{eff}}(z)]\}\right). \tag{10}$$

Minimizing free energy (10) with respect to $z_{\min}$ leads to the following self-consistence equation for $z_{\min}$,

$$z_{\min}=\frac{\int_0^{z_d} z\,\exp[-8(z_{\min}-z)^2-\bar{V}^{\text{eff}}(z)]dz}{\int_0^{z_d}\exp[-8(z_{\min}-z)^2-\bar{V}^{\text{eff}}(z)]dz}. \tag{11}$$

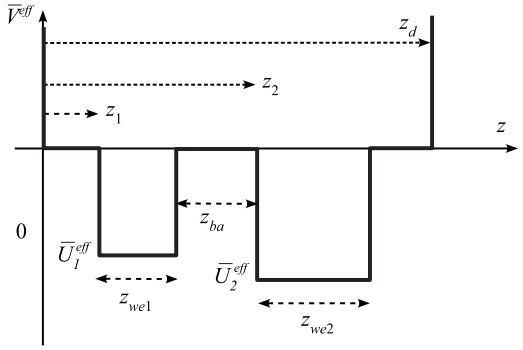

FIG. 3. Model potential for a membrane without repellers. The two wells representing the long and short stickers are separated by a potential barrier of width z_{ba}.

A. Membranes without repellers

Let us consider the effect of confinement, i.e., the finiteness of z_d, on the phase behavior of this system. For this purpose we first ignore repellers; i.e., we let $U_{ba}^{\text{eff}}=0$ (see also Fig. 3). The effect of repellers will be discussed later. Since the critical phenomenon for this system belongs to Ising universality class, for sufficiently strong potential depths the system is in two-phase state with two possible separations, one is closer to z_1, and another one is closer to z_2 [18]. For weak potential wells, the membrane can *tunnel* through the energy barrier between the wells and takes one average separation field $z_{\min}$.

As an example, Fig. 4 shows the relation between $\bar{U}_2^{\text{eff}}$ versus $z_{\min}$ given by Eq. (11) for $z_1=0.1$, $z_d=1.2$, $z_{we1}=z_{we2}=0.2$, and $z_{ba}=0.4$. The effective binding energy of type-1 stickers, $|\bar{U}_1^{\text{eff}}|$, is chosen to be $|\bar{U}_1^{\text{eff}}|=4$ for the upper curve and $|\bar{U}_1^{\text{eff}}|=|\bar{U}_{1c}^{\text{eff}}|=1.095$ for the lower curve. Intuitively, one expects that $z_{\min}$ increases as $|\bar{U}_2^{\text{eff}}|$ increases, and this is the case for $|\bar{U}_1^{\text{eff}}|\le|\bar{U}_{1c}^{\text{eff}}|$. However, when $|\bar{U}_1^{\text{eff}}|>|\bar{U}_{1c}^{\text{eff}}|$ there is a range of $\bar{U}_2^{\text{eff}}$ with multiple solutions for $z_{\min}$ which indicates two-phase coexistence and a first-order phase transition. The

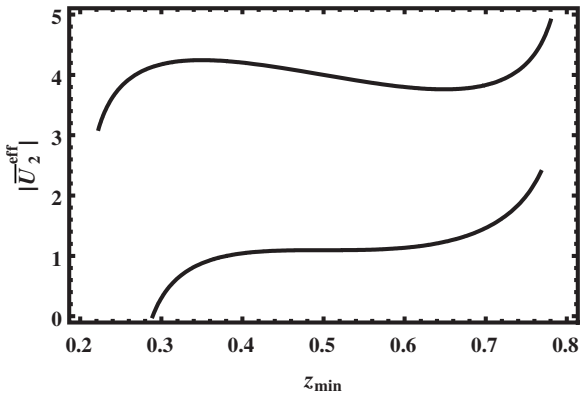

FIG. 4. The effective potential depth $|\bar{U}_2^{\text{eff}}|$ versus $z_{\min}$ for $z_1=0.1$, $z_d=1.2$, $z_{we1}=z_{we2}=0.2$, and $z_{ba}=0.4$. $|\bar{U}_1^{\text{eff}}|=4$ for the upper curve and $|\bar{U}_1^{\text{eff}}|=|\bar{U}_{1c}^{\text{eff}}|=1.095$ for the lower curve. The phase coexistence region for $|\bar{U}_1^{\text{eff}}|=4$ can be determined by Maxwell's equal-area construction.

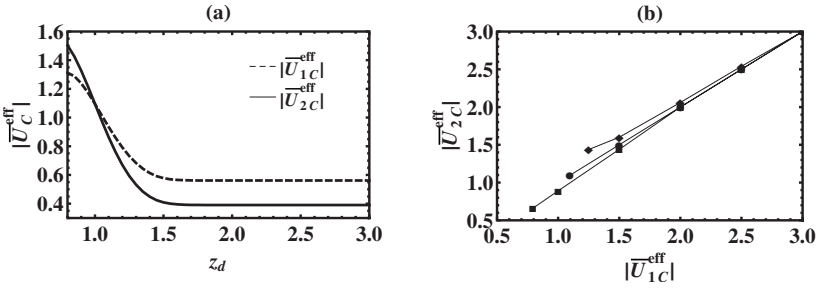

FIG. 5. (a) The critical potential depths versus z_d for $z_1=0.1$, $z_{ba}=0.4$, $z_{we1}=0.2$, and $z_{we2}=0.2$. When z_d is small, $|\bar{U}_{1c}^{\rm eff}|$ and $|\bar{U}_{2c}^{\rm eff}|$ increases as z_d decreases. (b) The phase coexistence curves for the system shown in (a). $z_d=0.9$ (top), $z_d=1$ (middle), and $z_d=1.2$ (bottom). Phase rich in type-2 stickers is suppressed as z_d decreases.

two-phase state ends at the critical point $(\bar{U}_{1C}^{\rm eff}, \bar{U}_{2C}^{\rm eff})$, which can be found by varying $\bar{U}_1^{\rm eff}$ until $\partial U_2^{\rm eff}/\partial z_{\rm min}$ and $\partial^2 U_2^{\rm eff}/\partial^2 z_{\rm min}$ have common zero for given z_1, z_d, z_{ba}, z_{we1}, and z_{we2}. The equation of state in the two-phase state, i.e., the relation between $\bar{U}_2^{\rm eff}$ and $z_{\rm min}$ for $|\bar{U}_1^{\rm eff}|>|\bar{U}_{1c}^{\rm eff}|$, and the phase coexistence curve can be obtained by Maxwell's equal-area construction [19].

To study such systems experimentally, one makes a lipid membrane that contains both long and short stickers which can adhere to the substrate, then put an upper surface to confine the height of the membrane. For given species of stickers, z_1, z_2, z_{we1}, and z_{we2} are fixed, although the binding energies between the stickers and the substrate are also fixed. $\bar{U}_1^{\rm eff}$ and $\bar{U}_2^{\rm eff}$ can be adjusted by changing the density of the stickers in the membrane. Thus the phase behavior of the system is determined by the two parameters $\bar{U}_1^{\rm eff}$ and $\bar{U}_2^{\rm eff}$. For systems with sufficiently strong effective binding energies, $\bar{U}_1^{\rm eff}$ and $\bar{U}_2^{\rm eff}$ depends on the relative strength of these effective binding energies, the membrane can have membrane height close to either $z_1+z_{we1}/2$ or $z_2+z_{we2}/2$, or the membrane can be phase separated into two domains, one with membrane height close to $z_1+z_{we1}/2$ and another one with membrane height close to $z_2+z_{we2}/2$. The two-phase state disappears as the effective binding energies of the stickers become weaker than the critical strengths $\bar{U}_{1c}^{\rm eff}$ and $\bar{U}_{2c}^{\rm eff}$, respectively. With Maxwell's equal-area construction, we can determine the phase boundaries and critical points for such systems. Figure 5(a) shows how the confinement affects the critical point $(\bar{U}_{1c}^{\rm eff}, \bar{U}_{2c}^{\rm eff})$ for $z_1=0.1$, $z_{ba}=0.4$, $z_{we1}=0.2$, and $z_{we2}=0.2$. The effect of confinement becomes important for $z_d \leq 1.5$, where $|\bar{U}_{1c}^{\rm eff}|$ and $|\bar{U}_{2c}^{\rm eff}|$ increase as z_d decreases. Thus we find that lateral phase separation induced by membrane adhesion is suppressed by compressing the membrane toward the substrate with an upper plate. This is because the entropic repulsion between the membrane and the hard wall located at z_d increases as z_d decreases, and the membrane is forced to tunnel through the barrier more often when z_d decreases. The phase coexistence curves for several magnitudes of z_d are shown in Fig. 5(b). Systems on the left side of the phase coexistence curves are richer in type-2 stickers (i.e., with greater $z_{\rm min}$) than systems on the right side of the phase coexistence curves. Besides the fact that the critical points shift toward greater $|\bar{U}_1^{\rm eff}|$ and $|\bar{U}_2^{\rm eff}|$ as z_d decreases, we also find that by decreasing z_d, the phase coexistence curves shift toward greater $|\bar{U}_{2c}^{\rm eff}|$. This is because smaller z_d enhance barrier crossing for the membrane to go from well 2 to well 1. Thus besides suppressing lateral phase separation, another effect of confinement is to suppress phase that is richer in type-2 stickers.

Mean-field theory is also convenient for studying how $\bar{U}_{1c}^{\rm eff}$ and $\bar{U}_{2c}^{\rm eff}$ vary as the length difference between the stickers changes. Figure 6(a) shows that when the effect of confinement is negligible, as the length difference between short and long stickers increases, lateral phase separation occurs at lower $|\bar{U}_{1c}^{\rm eff}|$ and $|\bar{U}_{2c}^{\rm eff}|$, as one expects. Furthermore, for $z_{we1}=z_{we2}$, $|\bar{U}_{1c}^{\rm eff}|>|\bar{U}_{2c}^{\rm eff}|$ due to collisions between the membrane and the substrate. On the other hand, Fig. 6(b) depicts that when $z_{we2}=1/2z_{we1}$, $|\bar{U}_{2c}^{\rm eff}|>|\bar{U}_{1c}^{\rm eff}|$ when z_{ba} is small due to the potential width difference. However, for large z_{ba} the steric repulsion between a membrane in the second well and the substrate becomes unimportant; thus $|\bar{U}_{2c}^{\rm eff}|<|\bar{U}_{1c}^{\rm eff}|$ even though $z_{we2}<z_{we1}$. These results demonstrate that our mean-field theory can be applied in analysis of various physical effects on the adhesion-induced lateral phase separation. A more detailed study will likely require time-consuming large-scale numerical simulations.

To check whether the physics revealed by our simple mean-field analysis holds when fluctuations are taken into account, we compare the mean-field result with Monte Carlo simulation. In the simulations partition function (4) is evaluated by the standard Metropolis algorithm [20,21] for mem-

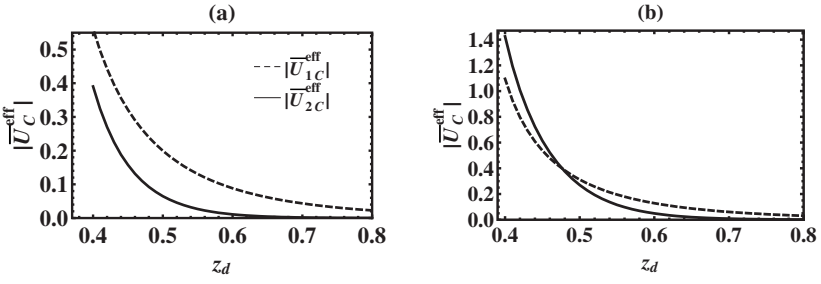

FIG. 6. (a) The critical potential depths versus z_{ba} for $z_1=0.1$, $z_d=6$, and $z_{we1}=z_{we2}=0.2$. $|\bar{U}_{1c}^{\rm eff}|>|\bar{U}_{2c}^{\rm eff}|$ for all z_{ba} and both $|\bar{U}_{1c}^{\rm eff}|$ and $|\bar{U}_{2c}^{\rm eff}|$ decrease as z_{ba} increases. (b) The critical potential depths versus z_{ba} for $z_1=0.1$, $z_d=6$, $z_{we1}=0.2$, and $z_{we2}=0.1$. $|\bar{U}_{2c}^{\rm eff}|>|\bar{U}_{1c}^{\rm eff}|$ for small z_{ba}, and $|\bar{U}_{1c}^{\rm eff}|>|\bar{U}_{2c}^{\rm eff}|$ for large z_{ba}.

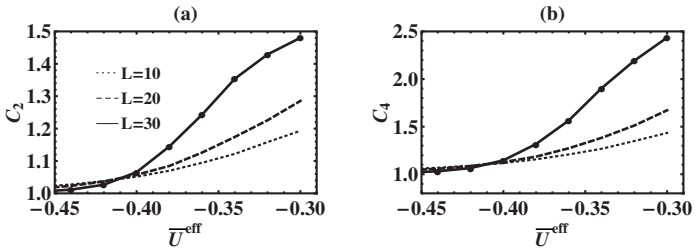

FIG. 7. (a) The cumulant C_2 versus $\bar{U}^{\rm eff}$ for $z_1=0.8$, $z_d=3.1$, $z_2=1.8$, $z_{we1}=z_{we2}=0.5$, and $z_{ba}=0.5$. The intersection point for $L=10$, $L=20$, and $L=30$ denotes the location of the critical potential depth $\bar{U}_C^{\rm eff}$. (b) The cumulant C_4 versus $\bar{U}^{\rm eff}$ for $z_1=0.8$, $z_d=3.1$, $z_2=1.8$, $z_{we1}=z_{we2}=0.5$, and $z_{ba}=0.5$.

branes of sizes $L=10\times 10$, $L=20\times 20$, and $L=30\times 30$. The simulation is performed with up to 10^8 attempted local moves per site.

When z_d and z_1 are both large, the effect of the walls is insignificant. Hence when $z_{we1}=z_{we2}$, the membrane is effectively in a symmetric double-well potential [17]. In this case, the critical potential depths $\bar{U}_{1c}^{\rm eff}=\bar{U}_{2c}^{\rm eff}=\bar{U}^{\rm eff}$ can be obtained from Binder cumulants $C_2=\langle \bar{z}^2\rangle/\langle|\bar{z}|\rangle^2$ and $C_4=\langle \bar{z}^4\rangle/\langle \bar{z}^2\rangle^2$. $\bar{z}=\frac{1}{N}\Sigma_{i=1}^{N}$ designates the spatial average of the separation field, while $\langle\cdots\rangle$ represents thermal average. When the potential barrier between the wells that represent the stickers is very low, the correlation length ξ of membrane height is small compared to system size L, and $C_2=\pi/2$ and $C_4=3$. When the barrier between the wells is very high, again $\xi\ll L$ but the cumulants take different limiting values: $C_2=1$ and $C_4=1$. When the system is located at the critical point, ξ diverges and C_2 and C_4 take values between these limiting cases, and these values are independent of system size L. Therefore the critical point can be found from the common intersection points of the cumulants C_2 and C_4 at different values of L [21]. As an example, Figs. 7(a) and 7(b) show C_2 and C_4 versus $\bar{U}^{\rm eff}$ for $z_1=0.8$, $z_d=3.1$, $z_2=1.8$, $z_{we1}=z_{we2}=0.5$, and $z_{ba}=1.2$. It is clear that the critical point is located at $\bar{U}^{\rm eff}\approx -0.41$.

The effect of confinement on lateral phase separation of membrane is important when z_d is small. In this case the walls affect the phase coexistence curve and the critical potential depths. Thus the phase coexistence curve and the critical potential depths in the simulations are determined by measuring the binding probability P_1 of the membrane in well 1, and the binding probability P_2 of the membrane in well 2. Membranes of size $L=120\times 120$ patches are simulated and the simulation is performed with up to 10^7 Monte Carlo steps. The simulation starts in the regime when both potential wells are deep and the membrane stays in well 2. Then we decrease $|\bar{U}_2^{\rm eff}|$; P_2 decreases continuously until the membrane switches from well 2 to well 1. This discontinuous transition signals a first-order phase transition [22]. The location of the critical point can be determined by repeating the above procedure for systems with progressively smaller $|\bar{U}_1^{\rm eff}|$. Below the critical point, the plot P_2 versus $\bar{U}_2^{\rm eff}$ is continuous.

Figure 8 shows the phase coexistence curves from Monte Carlo simulations for $z_1=0.1$, $z_{ba}=0.4$, $z_{we1}=0.2$, and $z_{we2}=0.2$. Similar to the phase coexistence curves constructed by mean-field theory, for small z_d the critical points are located at greater potential depths, and the phase coexistence curves shift toward greater $|\bar{U}_{2c}^{\rm eff}|$ in the vicinity of the critical points as membrane confined in well 2 feels higher entropic repulsion with the hard wall at z_d than membrane confined in well 1. Thus although quantitatively the critical points in the simulations are located at higher $|\bar{U}_1^{\rm eff}|$ and $|\bar{U}_2^{\rm eff}|$ than those in the mean-field theory due to fluctuations, simulations also show that confinement suppresses phase separation and confinement suppresses the phase that is richer in type-2 stickers. Thus, although mean-field theory cannot provide accurate prediction of the critical points, it provides good prediction about the shape of phase boundary in $|\bar{U}_1^{\rm eff}|-|\bar{U}_2^{\rm eff}|$ plane and the entropic effect of confinement on the phase boundary.

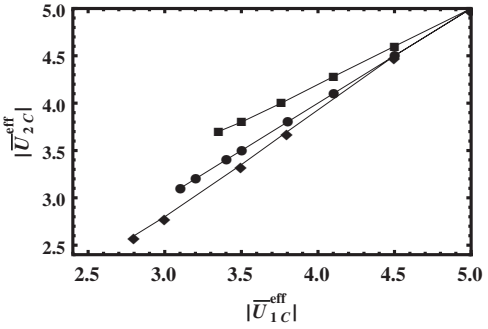

FIG. 8. Phase coexistence curves in $\bar{U}_1^{\rm eff}\bar{U}_2^{\rm eff}$ space constructed from Monte Carlo simulations for membranes without repellers. In the simulations $z_1=0.1$, $z_{ba}=0.4$, $z_{we1}=0.2$, and $z_{we2}=0.2$. $z_d=0.9$ (top), $z_d=1$ (middle), and $z_d=1.2$ (bottom).

B. Membranes with repellers

Now we discuss the effect of repellers on adhesion-induced lateral phase separation. First notice that adding repellers to a system means for given sticker species and densities (U_1, μ_1, U_2, and μ_2 are not changed), repellers with given U_3, μ_3, and l_3 are added to the system. Therefore we need to see how effective potentials associated with the stickers change as repellers are added to the system.

For membranes containing repellers, the effective potential of the membrane takes the form

$$\bar{V}^{\rm eff}=\begin{cases}\bar{U}_{ba}^{\rm eff} & \text{for } 0<z<z_1\\ \bar{U}_1^{\rm eff}\equiv[\bar{U}_1^{\rm eff}]_{\rm trans} & \text{for } z_1<z<z_1+z_{we1}\\ \bar{U}_{ba}^{\rm eff} & \text{for } z_1+z_{we1}<z<z_2\\ \bar{U}_2^{\rm eff}\equiv[\bar{U}_2^{\rm eff}]_{\rm trans} & \text{for } z_2<z<z_2+z_{we2}\\ \bar{U}_{ba}^{\rm eff} & \text{for } z_2+z_{we2}<z<z_3\\ 0 & \text{for } z_3<z<z_d,\end{cases} \tag{12}$$

as shown in Fig. 9. Here $\bar{U}_1^{\rm eff}<0$ and $\bar{U}_2^{\rm eff}<0$, while $\bar{U}_{ba}^{\rm eff}>0$.

The presence of repellers contributes to the effective potentials of the stickers in Eq. (12). To make this point more

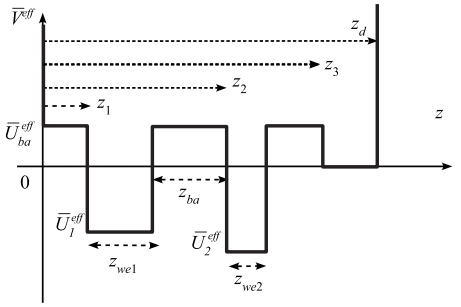

FIG. 9. Schematic potential for a membrane with short stickers, long stickers, and repellers. The membrane is confined between $z=0$ and $z=z_d$. There are two square wells of depths $|\bar{U}_1^{\rm eff}|$ and $|\bar{U}_2^{\rm eff}|$ and widths z_{we1} and z_{we2}, and one barrier of height $\bar{U}_{ba}^{\rm eff}$ due to the repellers.

transparent, let the effective potentials of sticker i ($i=1$ or 2) in the absence of repellers be

$$[\bar{U}_1^{\rm eff}]_0 = -T\ln\frac{1+e^{(-U_1+\mu_1)/T}+e^{\mu_2/T}}{1+e^{\mu_1/T}+e^{\mu_2/T}}, \tag{13}$$

and

$$[\bar{U}_2^{\rm eff}]_0 = -T\ln\frac{1+e^{\mu_1/T}+e^{(-U_2+\mu_2)/T}}{1+e^{\mu_1/T}+e^{\mu_2/T}}. \tag{14}$$

In the presence of repellers, the effective potentials become

$$[\bar{U}_1^{\rm eff}]_{\rm trans} = -T\ln\frac{1+e^{(-U_1+\mu_1)/T}+e^{\mu_2/T}+e^{\mu_3/T}}{1+e^{\mu_1/T}+e^{\mu_2/T}+e^{\mu_3/T}}, \tag{15}$$

$$[\bar{U}_2^{\rm eff}]_{\rm trans} = -T\ln\frac{1+e^{\mu_1/T}+e^{(-U_2+\mu_2)/T}+e^{\mu_3/T}}{1+e^{\mu_1/T}+e^{\mu_2/T}+e^{\mu_3/T}}, \tag{16}$$

and the effective potential of the repellers is

$$\bar{U}_{ba}^{\rm eff} = -T\ln\frac{1+e^{\mu_1/T}+e^{\mu_2/T}+e^{(-U_3+\mu_3)/T}}{1+e^{\mu_1/T}+e^{\mu_2/T}+e^{\mu_3/T}}. \tag{17}$$

Intuitively, adding repellers to the system reduces the affinity of the stickers; this can verified by straightforward algebra. Indeed, from Eqs. (13)–(16), one finds

$$|[\bar{U}_1^{\rm eff}]_{\rm trans}| = |[\bar{U}_1^{\rm eff}]_0| + T\ln\frac{1+e^{\mu_3/T}/[1+e^{(-U_1+\mu_1)/T}+e^{\mu_2/T}]}{1+e^{\mu_3/T}/(1+e^{\mu_1/T}+e^{\mu_2/T})} < |[\bar{U}_1^{\rm eff}]_0|, \tag{18}$$

and

$$|[\bar{U}_2^{\rm eff}]_{\rm trans}| = |[\bar{U}_2^{\rm eff}]_0| + T\ln\frac{1+e^{\mu_3/T}/[1+e^{\mu_1/T}+e^{(-U_2+\mu_2)/T}]}{1+e^{\mu_3/T}/(1+e^{\mu_1/T}+e^{\mu_2/T})} < |[\bar{U}_1^{\rm eff}]_0|, \tag{19}$$

because $U_1<0$ and $U_2<0$.

The above discussion suggests that to see if the presence of repellers enhances or suppresses adhesion-induced lateral phase separation of different species of stickers, one needs to compare the critical potentials $|\bar{U}_{ic}^{\rm eff}|$ in the presence of repellers with $|[\bar{U}_{ic}^{\rm eff}]_{\rm trans}|$, the potentials that are transformed from $|[\bar{U}_{ic}^{\rm eff}]_0|$ by Eqs. (18) and (19).

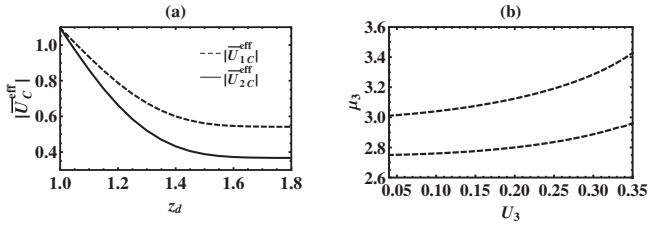

FIG. 10. (a) The critical potential depths versus z_d for $z_1=0.1$, $z_3=1.0$, $z_{ba}=0.4$, $z_{we1}=0.2$, $z_{we2}=0.2$, and $|\bar{U}_{ba}^{\rm eff}|=0.1$. For small z_d, $|\bar{U}_c^{\rm eff}|$ decreases as z_d increases. (b) Upper curve: $|\bar{U}_{2c}^{\rm eff}|-|[\bar{U}_{2c}^{\rm eff}]_{\rm trans}|=0$; lower curve: $|\bar{U}_{1c}^{\rm eff}|-|[\bar{U}_{1c}^{\rm eff}]_{\rm trans}|=0$. On the left of the curves, repellers suppress lateral phase separation; on the right of the curves, repellers enhance lateral phase separation; between the curves, $|\bar{U}_{2c}^{\rm eff}|-|[\bar{U}_{2c}^{\rm eff}]_{\rm trans}|<0$ and $|\bar{U}_{1c}^{\rm eff}|-|[\bar{U}_{1c}^{\rm eff}]_{\rm trans}|>0$. The curves are plotted for $z_1=0.1$, $z_3=1$, $z_d=2$, $z_{we1}=0.2$, $z_{we2}=0.2$, and $z_{ba}=0.4$.

As demonstrated in Sec. III A, although quantitatively not accurate, mean-field approximation gives us correct physical picture of the system under consideration. Since the precise magnitude of the critical potential depths is not the key issue of this section, we use mean-field theory to study the effect of repellers. First we check if the effect of confinement in the presence of repellers is the same as that in the absence of repellers. The critical potential depths in the presence of repellers versus z_d for $z_1=0.1$, $z_3=1.0$, $z_{ba}=0.4$, $z_{we1}=0.2$, $z_{we2}=0.2$, and $|\bar{U}_{ba}^{\rm eff}|=0.1$ in the mean-field approximation are shown in Fig. 10(a). Indeed, like the no-repeller case, the critical potential depths $|\bar{U}_{1c}^{\rm eff}|$ and $|\bar{U}_{2c}^{\rm eff}|$ decrease as z_d increases. Furthermore, the confinement effect is negligible for large values of z_d; this is also the same as no-repeller case.

To see the effect of repellers on adhesion-induced phase separation, we compare the numerical solutions of the critical potentials of the stickers $|[\bar{U}_{ic}^{\rm eff}]|$ with $|[\bar{U}_{ic}^{\rm eff}]_{\rm trans}|$. Figure 10(b) shows the curves on which $|\bar{U}_{ic}^{\rm eff}|=|[\bar{U}_{ic}^{\rm eff}]_{\rm trans}|$ for $z_1=0.1$, $z_d=6$, $z_{we1}=z_{we2}=0.2$, and $z_{ba}=0.4$. In Fig. 10(b), repellers suppress phase separation on the left of the curves, and enhance phase separation on the right of the curves. Between the curves $|\bar{U}_{2c}^{\rm eff}|-|[\bar{U}_{2c}^{\rm eff}]_{\rm trans}|<0$, and $|\bar{U}_{1c}^{\rm eff}|-|[\bar{U}_{1c}^{\rm eff}]_{\rm trans}|>0$. This indicates that repellers with stronger repulsive potential enhance, while repellers with weaker repulsive potential suppress adhesion-induced lateral phase separation. Although there is no analytical expression for the critical strengths of U_3 and μ_3 for the repellers to enhance lateral phase separation, the effect of repellers on the phase behavior of the system can be understood by the following simple analysis. When membrane-membrane collisions is not important, adding repellers should not significantly change the height of energy barrier between the wells of the stickers. Thus the critical potentials of the stickers in the presence of repellers are related to those in the absence of repellers by $|\bar{U}_{ic}^{\rm eff}|+\bar{U}_{ba}^{\rm eff}\approx|[\bar{U}_{ic}^{\rm eff}]_0|$. Repellers enhance phase separation as long as $|[\bar{U}_{ic}^{\rm eff}]_{\rm trans}|>|\bar{U}_{ic}^{\rm eff}|\approx|[\bar{U}_{ic}^{\rm eff}]_0|-\bar{U}_{ba}^{\rm eff}$. From Eqs. (17)–(19), this condition leads to

$$\ln\left[\frac{1+e^{\mu_3/T}/(1+e^{(-U_1+\mu_1)/T}+e^{\mu_2/T})}{1+e^{(-U_3+\mu_3)/T}/(1+e^{\mu_1/T}+e^{\mu_2/T})}\right]>0 \qquad (20)$$

for type-1 stickers. Since $U_3>0$, we find that at given μ_3 for sufficiently large U_3 the above inequality is satisfied; similarly when U_3 is sufficiently large, $|\bar{U}_{2c}^{\text{eff}}|-|[\bar{U}_{2c}^{\text{eff}}]_{\text{trans}}|<0$. Thus repellers with sufficiently strong repulsive potentials tend to enhance lateral phase separation.

IV. SUMMARY AND CONCLUSION

We have developed a mean-field analysis that is convenient for studying the phase behavior of membrane adhesion-induced lateral phase separation. Our study shows that vertical confinement tends to suppress adhesion-induced phase separation because long-sticker-rich state is suppressed due to the entropic loss. We also find that adding repellers reduces the effective binding energies of the stickers, and repellers play a nontrivial role in adhesion-induced phase separation: repellers with strong repulsive potential tend to enhance phase separation, whereas repellers with weak repulsive potential tend to suppress phase separation.

The main predictions of our theory are not difficult to check in experiments. For example, consider vesicle adhesion to supported membranes via two types of stickers. Our analysis predicts that it is possible to mix the phase-separated stickers by simply compressing the vesicle against the supporting substrate. The effect of repellers can be checked by incorporating nonadhesive flexible polymers and stiff rodlike molecules to the vesicle surface, and examining the adhesion zone. Flexible polymers should tend to suppress lateral phase separation, while stiff molecules should tend to enhance lateral phase separation. We believe that these effects could be useful in the development of new sensitive soft materials with possible applications in future biotechnologies.

ACKNOWLEDGMENTS

M.A. would like to thank Professor R. Lipowsky, T. R. Weikl, and B. Rozycki for discussions he had during his stay at Max Planck Institute for Colloids and Interfaces, Potsdam, Germany. M.A. would also like to thank the Asian Pacific Center for Theoretical Physics, Korea, as part of the paper was written during his visit there. This work was supported by National Science Council of Taiwan, Republic of China, under Grant No. NSC 96-2628-M-008-001-MY2.

[1] R. Lipowsky and E. Sackmann, *Structure and Dynamics of Membranes: Generic and Specific Interactions*, Handbook of Biological Physics Vol. 1B (Elsevier, Amsterdam, 1995).
[2] B. Alberts, A. Johnson, J. Lewis, M. Raff, K. Roberts, and P. Walter, *Molecular Biology of the Cell*, 3rd ed. (Garland, New York, 1994).
[3] S. Komura and D. Andelman, Eur. Phys. J. E **3**, 259 (2000).
[4] R. Bruinsma, A. Behrisch, and E. Sackmann, Phys. Rev. E **61**, 4253 (2000).
[5] A. Albersdfer, T. Feder, and E. Sackmann, Biophys. J. **73**, 245 (1997).
[6] T. R. Weikl, R. R. Netz, and R. Lipowsky, Phys. Rev. E **62**, R45 (2000).
[7] J. Nardi, T. Feder, and E. Sackmann, Europhys. Lett. **37**, 371 (1997).
[8] T. R. Weikl and R. Lipowsky, Phys. Rev. E **64**, 011903 (2001).
[9] H. Strey, M. Peterson, and E. Sackmann, Biophys. J. **69**, 478 (1995).
[10] D. Zuckerman and R. Bruinsma, Phys. Rev. Lett. **74**, 3900 (1995).
[11] C. R. F. Monks, B. A. Friedberg, H. Kupfer, N. Sciaky, and A. Kupfer, Nature (London) **395**, 82 (1998); G. Grakoui *et al.*, Science **285**, 221 (1999); D. M. Davis *et al.*, Proc. Natl. Acad. Sci. U.S.A. **96**, 15062 (1999).
[12] S. Y. Qi, J. T. Groves, and A. K. Chakraborty, Proc. Natl. Acad. Sci. U.S.A. **98**, 6548 (2001).
[13] N. J. Burroughs and C. Wülfing, Biophys. J. **83**, 1784 (2002).
[14] T. R. Weikl and R. Lipowsky, Biophys. J. **87**, 3665 (2004).
[15] H.-Y. Chen, Phys. Rev. E **67**, 031919 (2003).
[16] J.-Y. Wu and H.-Y. Chen, Phys. Rev. E **73**, 011914 (2006).
[17] M. Asfaw, B. Rozycki, R. Lipowsky, and T. R. Weikl, Europhys. Lett. **76**, 703 (2006).
[18] R. Lipowsky, J. Phys. II **4**, 1755 (1994).
[19] K. Huang, *Statistical Mechanics*, 2nd ed. (Wiley, New York, 1987).
[20] A. Ammann and R. Lipowsky, J. Phys. II **6**, 255 (1996).
[21] K. Binder and D. W. Heermann, *Monte Carlo Simulation in Statistical Physics* (Springer, Berlin, 1992).
[22] M. Asfaw, Ph.D. thesis, Max Planck Institute for Colloids and Interfaces, 2005 (unpublished).